Am J Physiol Endocrinol Metab 299: E695–E705, 2010.
First published May 25, 2010; doi:10.1152/ajpendo.00038.2010.

The unfolded protein response is activated in skeletal muscle by high-fat feeding: potential role in the downregulation of protein synthesis

Louise Deldicque,[1] Patrice D. Cani,[2] Andrew Philp,[3] Jean-Marc Raymackers,[1] Paul J. Meakin,[4] Michael L. J. Ashford,[4] Nathalie M. Delzenne,[2] Marc Francaux,[1] and Keith Baar[3]

[1]*Institute of Neurosciences, Research Group in Muscle Exercise and Physiology, UCLouvain, Louvain-la-Neuve;* [2]*Louvain Drug Research Institute, Unité de pharmacocinétique, métabolisme, nutrition et toxicologie, UCLouvain, Brussels, Belgium;* [3]*Division of Molecular Physiology, College of Life Sciences, and* [4]*Biomedical Research Institute, Ninewells Hospital and Medical School, University of Dundee, Dundee, Scotland, United Kingdom*

Submitted 14 January 2010; accepted in final form 24 May 2010

Deldicque L, Cani PD, Philp A, Raymackers JM, Meakin PJ, Ashford ML, Delzenne NM, Francaux M, Baar K. The unfolded protein response is activated in skeletal muscle by high-fat feeding: potential role in the downregulation of protein synthesis. *Am J Physiol Endocrinol Metab* 299: E695–E705, 2010. First published May 25, 2010; doi:10.1152/ajpendo.00038.2010.—High-fat diets are known to decrease muscle protein synthesis, the adaptation to overload, and insulin sensitivity. Conditions that disrupt endoplasmic reticulum (ER) homeostasis lead to the activation of the unfolded protein response (UPR) that is associated with decreases in protein synthesis, chronic inflammation, and insulin resistance. The purpose of the present study was to establish whether ER stress is induced by a high-fat diet in skeletal muscle and whether ER stress can decrease mTORC1 activity and protein synthesis in muscle cells. Two independent protocols of high-fat feeding activated the UPR in mice. In the first study, mice consuming a high-fat diet containing 70% fat and <1% carbohydrates for 6 wk showed higher markers of the UPR (BiP, IRE1α, and MBTPS2) in the soleus and in the tibialis anterior muscles and ATF4 in the tibialis anterior ($P < 0.05$). In the second study, a 20-wk high-fat diet containing 46% fat and 36% carbohydrates also increased BiP, IRE1α, and phospho-PERK protein and the expression of ATF4, CHOP, and both the spliced and unspliced forms of XBP1 in the plantar flexors ($P < 0.05$). In C_2C_{12} muscle cells, tunicamycin, thapsigargin, and palmitic acid all increased UPR markers and decreased phosphorylation of S6K1 ($P < 0.05$). Collectively, these data show that a high-fat diet activates the UPR in mouse skeletal muscle in vivo. In addition, in vitro studies indicate that palmitic acid, and other well-known ER stress inducers, triggered the UPR in myogenic cells and led to a decrease in protein synthesis and mTORC1 activity.

endoplasmic reticulum stress; binding protein; X box binding protein-1; ribosomal protein S6 kinase; protein synthesis

A HIGH-FAT DIET IS KNOWN to affect the physiology of skeletal muscle: preventing skeletal muscle hypertrophy in response to loading (39). It is possible that, over time, decreased load-induced muscle protein synthesis would result in a decrease in lean body mass and, as a result, a decrease in the capacity to take up and oxidize glucose, contributing to insulin resistance and the metabolic syndrome. Even though some hypotheses have been formulated to explain how a high-fat diet could affect muscle protein synthesis, no definitive mechanism has been presented. What is clear is that following a high-fat diet there is a decrease in ribosomal biogenesis and in the activation of mammalian target of rapamycin complex 1 (mTORC1) in response to overload (39).

The endoplasmic reticulum (ER) is where folding and post-translational modifications of proteins occur. Certain conditions, such as high lipids, glucose deprivation, or increased synthesis of secretory proteins disrupt ER homeostasis and lead to the accumulation of unfolded or misfolded proteins within the ER lumen (54). To cope with this, cells activate the unfolded protein response (UPR), a series of events that serve to restore ER function (21, 23, 35, 48). The UPR has three main effectors: ATF6 (activating transcription factor 6), IRE1α (inositol-requiring enzyme 1α), and PERK (protein kinase R-like ER protein kinase). In the basal (inactive) state, each of these factors associates with the protein chaperone BiP/GRP78 (binding protein/glucose-regulated protein-78), a member of the Hsp70 (heat shock protein-70) family. Upon accumulation of unfolded/misfolded proteins, ATF6, IRE1α, and PERK are released from BiP/GRP78 and become activated. The downstream effect of ATF6, IRE1α, and PERK release is the induction of genes, such as XBP1 (X box binding protein-1), CHOP [CCAAT/enhancer binding protein (C/EBP) homologous protein], and ATF4 (activating transcription factor 4), which lead to a decrease in protein synthesis and increase in protein folding capacity. When the unfolded protein response fails, the result is cell death, mostly in the form of apoptosis (19). Activation of the PERK-eIF2α-ATF4, the IRE1α-XBP1, and the ATF6 pathways upregulates the transcription factor CHOP, which in turn downregulates Bcl-2 (B-cell leukemia/lymphoma 2) expression, resulting in mitochondrial cytochrome *c* release (19). In addition, IRE1α-ASK1(apoptosis signal-regulating kinase-1)-JNK signaling activates the pro-apoptotic Bcl-2 family member BIM while inhibiting the antiapoptotic protein Bcl-2 (49). IRE1α activation also triggers the recruitment of caspase-12, a protein with homology to the caspase family of cysteine proteases involved in apoptosis and inflammatory cytokine processing (50).

Whereas ER stress has been widely studied in pancreatic islets, liver, and adipose tissue, where it has been proposed to be involved in the pathogenesis of diabetes (7, 10, 15, 37, 41), much less information exists about ER stress in skeletal muscle. In muscle, ER stress has been observed in myopathies such as myotonic dystrophy type 1 (13) and sporadic inclusion body myositis (26, 47). In addition, ER stress can be triggered by proinflammatory cytokines and lipids (33, 53). Since both of these factors are increased in obesity and diabetes, it is possible that ER stress may be activated in pathological metabolic conditions, leading to muscle wasting and further dysfunction

Address for reprint requests and other correspondence: K. Baar, Dept. of Neurobiology, Physiology and Behavior, Univ. of California, Davis, One Shields Ave., 181 Briggs Hall, Davis, CA 95616 (e-mail: kbaar@ucdavis.edu).

(32). In fact, a recent study in diabetic patients indicated that markers of the UPR were increased in cells isolated from muscle biopsies and cultured in the presence of palmitate (34), suggesting that ER stress is present in muscle in vivo, although this has yet to be shown. Even though there are suggestions that ER stress is induced in vivo, at least one study reported that ER stress markers were not altered in skeletal muscle of obese and high-fat-fed animals compared with controls (29).

Due to the important role of skeletal muscle in whole body metabolic regulation and the possibility that ER stress can regulate protein synthesis, muscle size, and insulin resistance, we sought to establish whether ER stress was induced by a high-fat diet and whether ER stress would decrease protein synthesis and mTORC1 activity. Therefore, we first tested whether the unfolded protein response was increased in mouse skeletal muscle after two different high-fat diet protocols. Second, we determined the effect of agents known to induce ER stress (9, 29, 36, 40, 46), such as tunicamycin, thapsigargin and palmitic acid on mTORC1 activity and protein synthesis in C_2C_{12} muscle cells.

MATERIALS AND METHODS

Protocols

Cell cultures. C_2C_{12} murine skeletal muscle myoblasts (ATCC) were seeded in 150-mm-diameter culture dishes and grown in Dulbeccos's modified Eagle medium (DMEM, Life Technologies) supplemented with 10% fetal bovine serum and 1% penicillin-streptomycin (5,000 U/5,000 μg/ml). Cells were then plated in six-well plates until reaching 90% confluence. At that time, the proliferation medium was replaced with a differentiation medium containing 2% horse serum and 1% penicillin-streptomycin (5,000 U/5,000 μg/ml). After 96 h of differentiation, tunicamycin (TN, 1 μg/ml), thapsigargin (TG, 200 nM), or palmitic acid (PA, 1 mM) plus 2% BSA was added for 17 h. TN and TG are well-documented chemical inducers of ER stress by blocking *N*-glycosylation and calcium entry into the ER, respectively, and were used as positive controls. At the end of the incubation period, cells were harvested, and cell lysates were immediately frozen at −80°C for subsequent analyses. All experiments were performed three times in triplicates except the dose-response curves to PA.

Animal Studies. STUDY 1. Eight-week-old female C57BL/6J mice (Laboratory of Experimental Surgery, UCLouvain, Belgium) were housed in groups of seven per cage at 22°C on a 12:12-h light-dark cycle and were given free access to diet and water. After 1 wk of acclimation, mice were randomly assigned to either a control group (Ctrl-1, $n = 7$) or a high-fat diet group (HFD-1, $n = 7$). The control group ate standard chow, whereas the other group received a diet containing 49.5 g fat (corn oil and lard)/100 g, 37 g protein (cow milk casein)/100 g, and <1 g carbohydrate/100 g. This represents in percent total energy: 72% fat, 28% protein, and <1% carbohydrate (UAR). This diet is known to induce a marked diabetic and metabolic stress state (3, 4). At the end of the 6 wk, 6-h-fasted mice were terminally anesthetized by intraperitoneal injection of pentobarbital sodium solution (using 60 mg/kg body wt, Nembutal, Sanofi). Tibialis anterior and soleus muscles were removed as fast as possible and immediately frozen in liquid nitrogen. All mouse experiments were approved by the local ethics committee, and the housing conditions were as specified by the Belgian Law of November 14, 1993, on the protection of laboratory animals (Agreement no. LA 1220548).

STUDY 2. Eighteen- to twenty-wk-old C57BL/6J mice (Charles River, UK) were housed at 22°C on a 12:12-h light-dark cycle and were given free access to diet and water. Mice were randomly assigned to either a control group (Ctrl-2, $n = 12$) or a HFD group (HFD-2, $n = 19$). The control group ate standard chow (RM1, Special Diets Services), whereas the other group received a diet containing 23.6 g fat (lard and soybean oil)/100 g, 21.3 g protein (casein)/100 g, and 41.2 g carbohydrate/100 g (58V8, Test Diet). This represents in percent total energy: 46% fat, 18% protein, and 36% carbohydrate. At the end of the 20 wk, the mice were starved overnight prior to being culled with an overdose of Euthatal (Merial Animal Health). Plantar flexor muscles were removed as fast as possible and immediately frozen in liquid nitrogen. All procedures conformed to the UK Animals (Scientific Procedures) Act 1986 and were approved by the ethical review committee of the University of Dundee (UK).

Protein extraction, SDS/PAGE, and immunoblotting. Cells were rinsed once with PBS and harvested in a lysis buffer containing 20 mM Tris, pH 7.0, 270 mM sucrose, 5 mM EGTA, 1 mM EDTA, 1% Triton X-100, 1 mM sodium orthovanadate, 50 mM sodium β-glycerophosphate, 5 mM sodium pyrophosphate, 50 mM sodium fluoride, 1 mM DTT, and a protease inhibitor cocktail containing 1 mM EDTA (Roche Applied Science). Frozen muscles were ground in a mortar and homogenized as previously described (5a). The homogenates were then centrifuged for 10 min at 10,000 *g*, and the supernatants were immediately stored at −80°C. Protein concentration was determined using the DC protein assay kit (Bio-Rad Laboratories).

Cell lysates (15 μg for cell culture proteins and 60 μg for skeletal muscle proteins) were combined with Laemmli sample buffer and separated by SDS-PAGE. After electrophoretic separation at 40 mA for 1 h, the proteins were transferred to a PVDF membrane at 80 V for 2 h for Western blot analysis. Membranes were then incubated in a 5% Blotto solution. Subsequently, membranes were incubated with the following antibodies overnight at 4°C: eEF2 (eukaryotic elongation factor 2), S6K1 (70-kDa ribosomal protein S6 kinase), phospho-S6K1 Thr^{389}, phospho-S6K1 Thr^{421}/Ser^{424}, BiP, PDI (protein disulfide isomerase), MBTPS2 (membrane-bound transcription factor protease site 2), IRE1α, phospho-PERK Thr^{980}, caspase-12, caspase-3, PARP (poly ADP-ribose polymerase), ATF6, and GAPDH (glyceraldehyde-3-phosphate dehydrogenase). All antibodies were from Cell Signaling, except the GAPDH was from Abcam, the ATF6 was from Imgenex, and the phospho-S6K1 Thr^{389}, phospho-S6K1 Thr^{421}/Ser^{424}, and S6K1 were from Santa Cruz Biotechnology.

Membranes were washed in TBS-T and incubated for 1 h at room temperature in a secondary antibody conjugated to horseradish peroxidase. After an additional three washes, chemiluminescence detection was carried out using an enhanced chemiluminescent Western blotting kit (ECL Plus, Amersham Biosciences). The films were then scanned on an ImageScanner using the Labscan software and quantified with the Image Master 1D Image Analysis software (Amersham Biosciences). Results are reported relative to eEF2 total for in vitro experiments and to GAPDH for in vivo experiments. Preliminary experiments show that eEF2 and GAPDH expressions did not change after the treatments. A value of 1 was arbitrarily assigned to the control conditions, which were used as a reference for the other conditions.

RNA extraction and quantitative real-time PCR. Total RNA from the cells of one 35-mm well (6-well plates) or from ~20 mg of frozen tissue samples was extracted with 1 ml of TriPure reagent (Roche) according to the instructions provided by the manufacturer (Roche Diagnostics). RNA was quantified by spectrophotometry (260 nm) and its concentration adjusted to 1 μg/μl by using RNase-free water. Since soleus muscles have low protein yields (~5–6 mg), the RNA concentrations obtained after extraction were too low to perform the reverse transcription reaction. For tibialis anterior and C_2C_{12} cells, cDNA was prepared by reverse transcription of 1 μg of total RNA using the reverse transcription system (Promega). SYBR Green was used for real-time PCR detection. Real-time PCR primers were designed (Table 1) for mouse CHOP, ATF4, spliced (s) XBP1, unspliced (u) XBP1, GAPDH, and RPL19 (ribosomal protein L19). Specific primers were designed to recognize the spliced, or active, form of XBP1 (XBP1s) vs. the unspliced form (XBP1u). GAPDH was

Table 1. *Sequences of primers used for mRNA quantification by real-time RT-PCR*

	Forward	Reverse
CHOP	CCT AGC TTG GCT GAC AGA GG	CTG CTC CTT CTC CTT CAT GC
ATF4	GAG CTT CCT GAA CAG CGA AGT G	TGG CCA CCT CCA GAT AGT CAT C
XBP1s	GAG TCC GCA GCA GGT G	GTG TCA GAG TCC ATG GGA
XBP1u	AAG AAC ACG CTT GGG AAT GG	ACT CCC CTT GGC CTC CAC
GAPDH	TGG AAA GCT GTG GCG TGA T	TGC TTC ACC ACC TTC TTG AT
RPL19	GAA GGT CAA AGG GAA TGT GTT CA	CCT TGT CTG CCT TCA GCT TGT

CHOP, CCAAT/enhancer binding protein homologous protein; ATF4, activating transcription factor 4; XBP1s and XBP1u, X box-binding protein-1, spliced and unspiced; RPL19, ribosomal protein L19.

used as the reference gene for in vitro experiments and RPL19 for in vivo experiments. All samples were run at least in duplicate in a single 96-well reaction plate, and the data were analyzed according to the $2^{-\Delta\Delta C_T}$ method. The identity and purity of the amplified product were checked through analysis of the melting curve carried out at the end of amplification. A value of 1 was arbitrarily assigned to the control condition to which the other conditions were reported.

Incorporation of [^{35}S]methionine/cysteine. Cells were maintained in serum-free DMEM while ER stress inducers were added for 17 h. ER stress inducers were maintained in culture medium during the whole experiment. Preliminary experiments confirm that the absence of serum did not modify the UPR induced by TN, TG, or PA. One hour before cell labeling, full DMEM was replaced with DMEM lacking methionine and cysteine. After that preincubation period, 3.66 μCi of a [^{35}S]methionine-cysteine mixture (EasyTag Express Protein Labeling Mix, NEN Life Science Products) was added to each well, and the cells were returned to the incubator for 2 h. Cells were then rinsed twice with PBS and lysed in a buffer containing 20 mM Tris pH 7.4, 150 mM NaCl, 1 mM Igepal C630 (NP-40), 10% glycerol, 50 mM β-glycerophosphate, 50 mM NaF, and a protease inhibitor cocktail. Cell lysates were centrifuged for 2 min at 10,000 *g*, and 15 μl of the supernatant was spotted on a Whatman paper in duplicate, whereas a 20-μl aliquot was saved to measure protein content in each sample. Whatman papers were washed three times in 5% trichloroacetic acid containing cold methionine and cysteine, rinsed once in ethanol, and dried at 37°C. Scintillating liquid (4 ml of Ultimagold, PerkinElmer) was then added to the papers, and ^{35}S incorporation was counted in a scintillation counter (Beckman) for 2 min. Protein content was measured with the DC protein assay (Bio-Rad) with BSA as standard. Results were reported in femtomoles per minute per milligram of protein. It should be specified that due to technical difficulties the actual specific activity of the precursor pool was not measured. It is possible that the uptake of ^{35}S was different between the treatment groups and that this contributed to the difference in protein synthesis.

Glucose tolerance test. STUDY 1. An oral glucose tolerance test (OGTT) (gavage with 1 mg glucose/g body wt; 20% glucose solution) was performed on 6-h-fasted mice at the end of the 6-wk treatment. Blood glucose was determined with a glucose meter (Roche Diagnostics) on 3.5 μl of blood collected from the tip of the tail vein 30 min before and 0, 15, 30, 60, 90, and 120 min following glucose injection.

STUDY 2. An intraperitoneal glucose tolerance test (IPGTT; injected with 2 mg glucose/g body wt; 25% glucose solution) was performed on 16-h-fasted mice at the end of the 20-wk treatment. Blood glucose was determined with a glucose meter (Bayer) on ~1 μl of blood collected from the tip of the tail vein at 0, 15, 30, 45, 60, and 120 min following glucose injection.

Cytokine quantification. Cytokine levels were determined in 12 μl of plasma using a kit (Bio-Plex Multiplex, Bio-Rad) and measured using Luminex technology (Bio-Plex).

Statistical Analysis

The effect of the different treatments was tested by unpaired Student's *t*-test except the effect of HFD on mass gain and glucose tolerance test. For these data, diet × time interactions were evaluated using a two-way analysis of variance for repeated measured (RM ANOVA). When appropriate, Student-Newman-Keuls post hoc tests were applied. The significance threshold was set to $P < 0.05$. Results are presented as means ± SE.

RESULTS

HFD-1 Increases Body Mass, Decreases Glucose Tolerance, and Induces Inflammation

During HFD-1, mice fed with a normal diet increased body mass by 20% (Fig. 1*A*). At the end of the 6 wk, HFD-1 mice weighed 10% more than control mice (Fig. 1*A*, $P < 0.001$). HFD-1 increased visceral fat content by 50% (Fig. 1*B*, $P < 0.05$) compared with control mice. Mice fed HFD-1 were glucose intolerant as indicated by the OGTT performed at the end of the 6 wk (Fig. 1*C*). For the same amount of glucose given orally, plasma glucose concentrations remained elevated

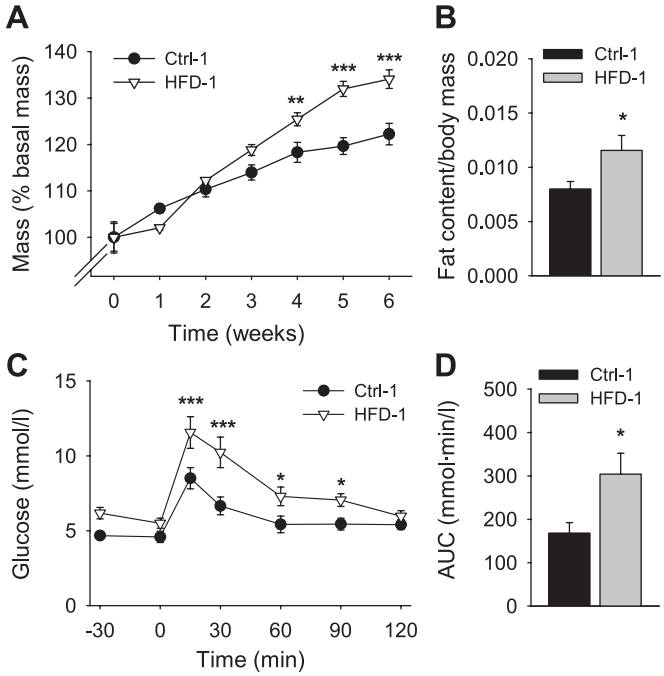

Fig. 1. Body mass, fat content, and oral glucose tolerance test (OGTT). *A*: mice were weighed weekly and their body mass was reported relative to basal value. *B*: at the end of the 6 wk, visceral fat content was precisely dissected and weighed and reported to body mass. *C* and *D*: OGTT was performed on 6-h-fasted mice at the end of the 6-wk treatment. *C*: plasma glucose concentrations 30 min before and 0, 15, 30, 60, 90, and 120 min after oral glucose load. *D*: area under curve (AUC) of glucose excursion after oral glucose load. Results are means ± SE. Ctrl-1, control 1; HFD-1, high-fat diet 1. $^*P < 0.05$, $^{**}P < 0.01$, $^{***}P < 0.001$ vs. Ctrl-1.

up to 90 min after gavage (Fig. 1*C*, $P < 0.05$), whereas plasma insulin concentrations were not different between groups (data not shown). The area under the curve was increased 1.8-fold by the HFD-1 (Fig. 1*D*, $P < 0.05$). Inflammation was assessed by measuring plasma levels of several pro- and anti-inflammatory cytokines (Table 2). HFD-1 increased IL-6 and IL-10 concentrations by 250% ($P < 0.05$). To confirm the inflammatory state at the tissue level, the phosphorylation state of JNK (c-Jun NH_2-terminal kinase) and IKK (I-κB kinase) were measured as well as the mRNA expression of IL-1 and IL-6 in muscles and liver. JNK and IKK/NF-κB (nuclear factor κ-light-chain enhancer of activated B-cells) have been implicated in insulin resistance and inflammation induced by ER stress through the IRE1α pathway (11, 15). Phospho-JNK and phospho-IKK were increased by HFD-1 in the soleus, and phospho-JNK was increased in the liver. IL-1 mRNA level was increased and IL-6 decreased by HFD-1 in the tibialis anterior [$P < 0.05$; Supplemental Fig. 1 (Supplemental materials are found in the online version of this paper at the Journal website)].

HFD-1 Increases the Expression of Proteins Involved in UPR

The UPR was measured in liver to ensure that ER stress was induced by high-fat feeding, as already described in the literature (28, 52). In the liver, the protein expression of PDI, IRE1α, MBTPS2, and the phosphorylation of PERK, as well as the mRNA expression of XBP1u, were more than doubled ($P < 0.05$; data not shown). Having shown that the UPR was induced by high-fat feeding in a tissue known to be responsive to ER stress, we determined whether the same response could be observed in skeletal muscle.

Several UPR markers were higher in skeletal muscles of HFD-1 than in control mice (Fig. 2). The changes were more pronounced in slow-type soleus muscle (Fig. 2*A*) than in fast-type tibialis anterior muscle (Fig. 2*C*). In the soleus (Fig. 2*A*), HFD increased the protein expression of BiP ($P < 0.05$) and MBTPS2 ($P < 0.001$), the enzyme that cleaves ATF6 into a functional transcription factor, eightfold and IRE1α ($P < 0.05$) fivefold. HFD also increased caspase-12 expression and the absolute amount of cleaved, and thus potentially active, caspase-12 (Fig. 2*B*, $P < 0.05$). However, the ratio between the cleaved and the total forms of caspase-12 after HFD was not different from control conditions in soleus.

In the tibialis anterior muscle (Fig. 2*C*), HFD-1 doubled BiP ($P < 0.05$) and IRE1α ($P < 0.05$) protein levels and tripled MBTPS2 ($P < 0.05$). At the transcriptional level, only ATF4 mRNA was increased (35%, $P < 0.05$; Fig. 2*E*). HFD had no effect on caspase-12 total expression but increased the absolute amount of cleaved caspase-12, making the ratio of cleaved to total caspase-12 significantly higher than in control conditions in tibialis anterior (Fig. 2*D*, $P < 0.05$). It is of note that, contrary to soleus muscle, cleaved caspase-12 was not detectable in control conditions in tibialis anterior (Fig. 2*D*), whereas total caspase-12 was observed.

Table 2. *Plasma cytokine concentrations*

	Ctrl-1	HFD-1
IL-1α	34 ± 11.3	20 ± 3.5
IL-1β	26 ± 6.2	18 ± 2.5
IL-6	22 ± 3.3	56 ± 11.3*
IL-10	43 ± 14.0	112 ± 24.3*
IL-15	306 ± 27.2	257 ± 17.8
IL-18	440 ± 107.7	593 ± 189.8
MCP-1	107 ± 13.1	120 ± 12.4
MIP-1α	139 ± 10.6	178 ± 18.7
TNF-α	26 ± 6.4	14 ± 1.2

Values are means ± SE. Ctrl-1, control 1; HFD-1, 6-wk high-fat diet; MCP-1, monocyte chemoattractant protein-1; MIP-1α, macrophage inflammatory protein-1α. *$P < 0.05$ vs. Ctrl-1.

HFD-2 Increases Body Mass And Decreases Glucose Tolerance

To determine whether the effects of a HFD on ER stress were specific to the 70% fat diet, we studied muscle from a second HFD experiment (HFD-2) using a lower percentage of fat (45%) for a longer period (20 wk). This diet was chosen as it is more representative of the diet in the developed world. Throughout the 20 wk of experiment, mice fed a normal diet increased body mass by 30% (Fig. 3*A*). At the end of the 20 wk, HFD-2 mice weighed 20% more than control mice (Fig. 3A, $P < 0.001$). HFD-2 almost doubled the percentage fat mass (Fig. 3*B*, $P < 0.001$) compared with control mice. Mice fed HFD-2 were glucose intolerant as indicated by the IPGTT performed at the end of the 20 wk (Fig. 3*C*, $P < 0.05$). The area under the curve was increased by 33% by the HFD-2 (Fig. 3*D*, $P < 0.05$).

45% HFD-2 Increases Expression of Proteins and mRNAs Involved in UPR

As observed after 70% HFD-1 for 6 wk, 45% HFD-2 for 20 wk increased several UPR markers in plantar flexor muscles (Fig. 4). HFD-2 increased the protein expression of BiP by 30% ($P < 0.05$), IRE1α by 200% ($P < 0.001$), and the phosphorylation of PERK by 50% ($P < 0.05$). Cleaved-to-total caspase-12 ratio tended to decrease in HFD-2 conditions without reaching the statistical threshold (Fig. 4*B*). HFD-2 had a more pronounced effect on the transcriptional regulation induced by the UPR (Fig. 4*C*). HFD-2 almost doubled ATF4 ($P < 0.001$) and CHOP mRNA ($P < 0.01$) and tripled both XBP1s and XBP1u forms ($P < 0.001$).

UPR Is Induced by TN, TG, and PA In C_2C_{12} Myogenic Cells

Since both HFDs induced markers of ER stress, we next sought to determine the effect of ER stress on muscle cell function. The UPR was strongly activated by TN, TG, and PA in C_2C_{12} cells (Fig. 5). After a 17-h incubation with these agents, BiP was increased more than 100-fold by TN and TG and more than 30-fold by PA (Fig. 5*A*, $P < 0.001$). IRE1α expression, which reflects the activation of the IRE1α pathway (44), doubled in TN and PA conditions and increased fivefold with TG (Fig. 5*A*, $P < 0.05$). Phosphorylation of PERK was increased 10-fold by TN and PA and 30-fold by TG (Fig. 5*A*, $P < 0.05$). ATF6 was reduced following PA incubation (Fig. 5*A*, $P < 0.01$).

ER stress inducers decreased caspase-12 total expression but increased the amount of cleaved caspase-12 except for PA, which only decreased caspase-12 total expression, making the ratio of cleaved to total caspase-12 significantly higher than in control conditions (Fig. 5*B*, $P < 0.05$).

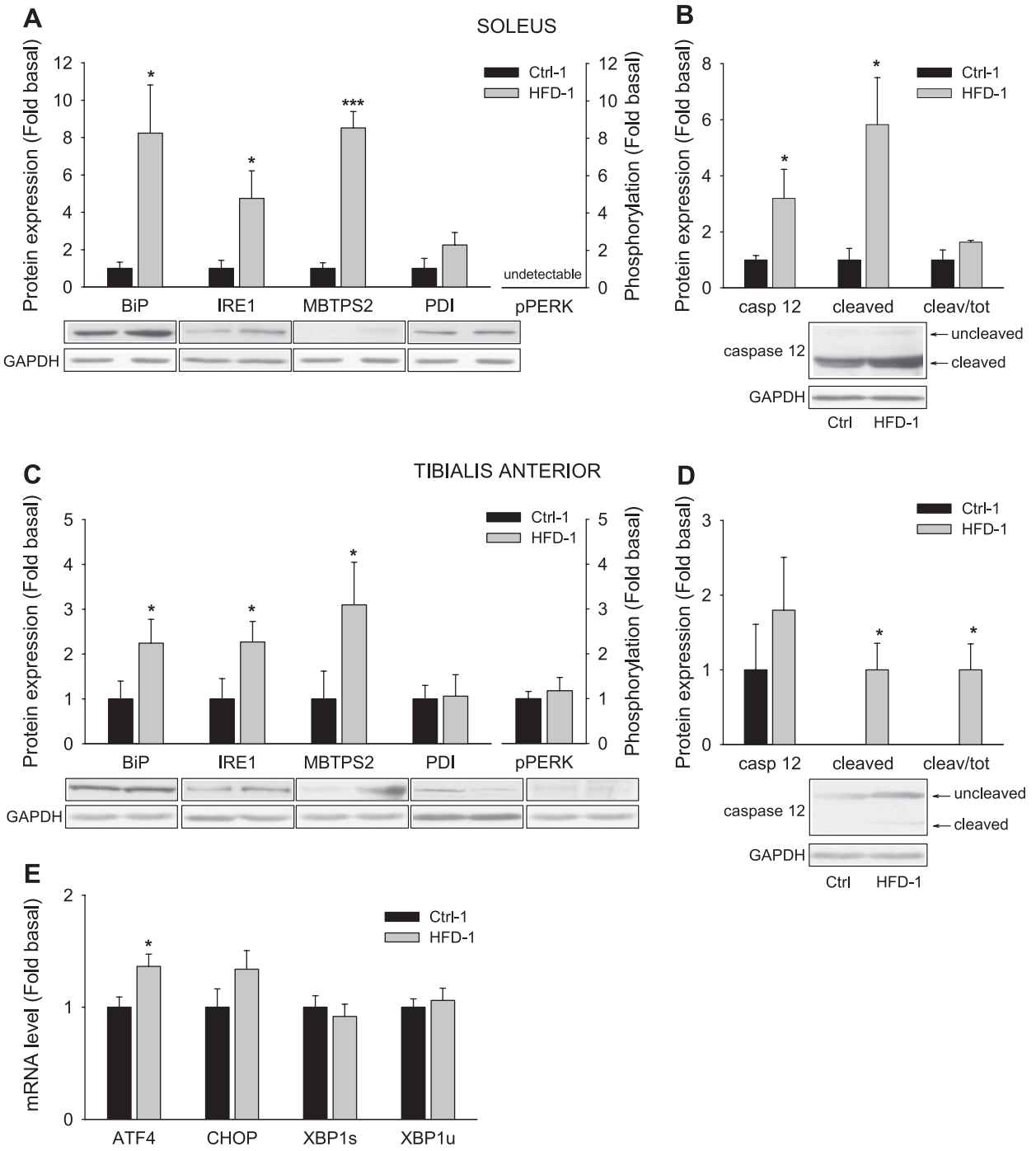

Fig. 2. 70% HFD-induced unfolded protein response (UPR) in mouse skeletal muscle. *A–D*: protein expression of BiP, IRE1α, MBTPS2, PDI, and phosphorylation of PERK (*A* and *C*) and caspase-12 expression and cleavage (*B* and *D*) in soleus and tibialis anterior muscles after 6-wk HFD-1. *E*: mRNA level of ATF4, CHOP, XBP1s, and XBP1u in tibialis anterior after 6-wk HFD-1. Results are means ± SE. A value of 1 was arbitrarily assigned to control conditions to which HFD-1 were reported and expressed as fold basal. BiP, binding protein; IRE1α, inositol-requiring enzyme 1α; MBTPS2, membrane-bound transcription factor protease site 2, PDI, protein disulfide isomerase; pPERK, phosphorylated protein kinase R-like endoplasmic reticulum (ER) protein kinase; GAPDH, glyceraldehyde-3-phosphate dehydrogenase; ATF4, activating transcription factor 4; CHOP, C/EBP (CCAAT/enhancer binding protein) homologous protein; XBP1s, spliced X box-binding protein-1; XBP1u, unspliced XBP1. $*P < 0.05$, $***P < 0.001$ vs. Ctrl-1.

Since ER stress induces responses at both the translational and the transcriptional levels, we also analyzed the mRNA levels of some well-documented transcriptional ER stress markers: CHOP, ATF4, and XBP1 (Fig. 5*C*) (10, 18). ATF4 mRNA was doubled by TN, TG, and PA ($P < 0.001$), and CHOP mRNA was increased 10-fold in response to PA and 30-fold with TN and TG ($P < 0.001$). XBP1s mRNA was 15-fold more abundant in TN and PA and 25-fold in TG than in control conditions (Fig. 5*C*, $P < 0.001$). The large increase in the mRNA of the active form of XBP1 contrasted with the more modest increase in the unspliced form induced by TN and TG and even the decrease observed in PA conditions (Fig. 5*C*,

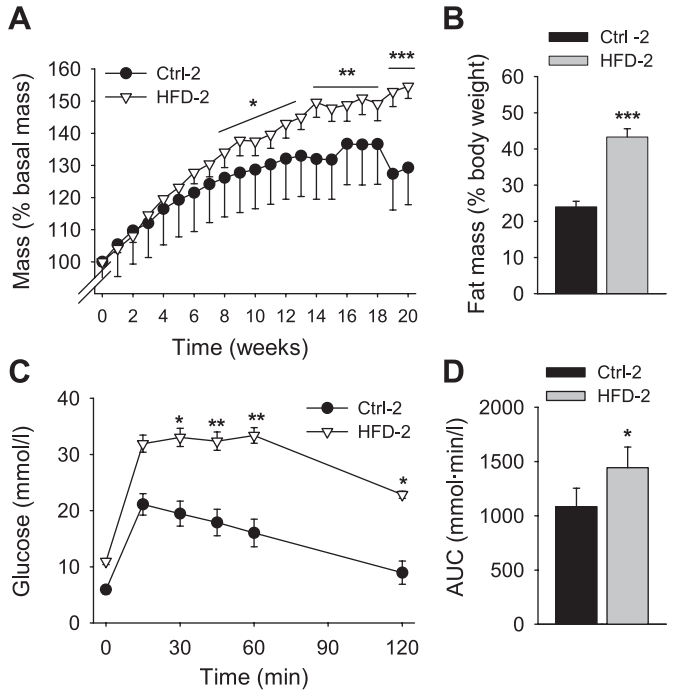

Fig. 3. Body mass, percent fat mass, and ip glucose tolerance test (IPGTT). *A*: mice were weighed weekly and their body mass was reported relative to basal value. *B*: at the end of 20 wk, %fat mass was measured by quantitative magnetic resonance. *C* and *D*: IPGTT was performed on 16-h-fasted mice at the end of the 20-wk treatment. *C*: plasma glucose concentrations 0, 15, 30, 45, 60, and 120 min after ip glucose injection. *D*: AUC of glucose excursion after ip glucose injection. Results are means ± SE. Ctrl-2, control 2; HFD-2, high-fat diet 2. $*P < 0.05$, $**P < 0.01$, $***P < 0.001$ vs. Ctrl-2.

$P < 0.001$). The latter result may be related to the decrease in ATF6 by PA, since the ATF6 pathway has been proposed as the regulator of the transcription of the unspliced form of XBP1, and IRE1α would make it active by enhancement of its splicing (51).

The percentages of cleaved caspase-3 and cleaved PARP were used as markers of apoptosis (Fig. 5*D*). No cleaved caspase-3 was detectable in Ctrl and PA conditions, whereas 1.0% in TN and 0.7% in TG of total caspase-3 were in the cleaved form ($P < 0.05$). In the same way, no cleaved PARP was detectable in Ctrl and PA conditions, whereas 3% and 8% of total PARP were in the cleaved form following TN and TG treatment, respectively ($P < 0.001$).

The effect of PA on the UPR is dose dependent, as at lower doses (250–500 μM) the UPR was not affected or even repressed, whereas at larger doses (750–1,000 μM) BiP, IRE1α, and phospho-PERK were increased (Fig. 5*E*).

PA Decreases Protein Synthesis in C_2C_{12} Myogenic Cells

PA did not affect the ability of insulin to increase 2-deoxyglucose (2-DG) uptake (data not shown) but decreased the rate of ^{35}S incorporation into proteins by 20% (Fig. 6*A*, $P < 0.001$). The decrease in protein synthesis suggested that mTORC1 activity might be altered by PA. As a marker of mTORC1 activity, we measured the phosphorylation of the mTORC1 site on S6K1. Treatment for 17 h with PA resulted in a 50% decrease in S6K1 phosphorylation at Thr^{389} (Fig. 6*B*, $P < 0.01$), indicating that mTORC1 activity was decreased by ER stress. To determine whether the effect of PA on mTORC1 could have been mediated by ER stress, the effect of both TN and TG on S6K1 phosphorylation was determined. As with PA, treatment with TN or TG decreased S6K1 phosphorylation, indicating that the effects of PA on mTORC1 activity could be mediated by the ER stress response. In high-fat-fed mice, S6K1 phosphorylation tended to increase (Fig. 6*C*). However, since the mice were in the fasted state, the mTORC1 site (Thr^{389}) was barely detectable, and the changes in S6K phosphorylation may be secondary to the altered hormonal milieu.

To determine the dynamics of the relationship between ER stress and mTORC1/S6K1, C_2C_{12} myogenic cells were incubated for 6 or 24-h with TN alone, insulin alone, or both TN and insulin (Fig. 6*D*). After 6 h, the phosphorylation of PERK and the expression of BiP were marginally increased by TN, whereas phospho-S6K1 (Thr^{389}) was increased by insulin even in the presence of TN. After 24 h, BiP was still increased, whereas PERK phosphorylation was not affected by TN. Phosphorylation of S6K1 by insulin at 24 h was repressed by TN. These data indicate that activation of the mTORC/S6K1 pathway by insulin does not induce ER stress in C_2C_{12} myogenic cells, whereas activation of the UPR represses the basal phosphorylation state of the mTORC/S6K1 pathway as well as its activation by insulin.

DISCUSSION

The main findings of the present study are *1*) that the UPR is activated in mouse skeletal muscle by an HFD and in C_2C_{12} cells by PA, and *2*) that ER stress can decrease protein synthesis and mTORC1 activity in muscle cells. This extends previous work in the pancreas and liver (6, 28, 52), suggesting that HFD results in ER stress in the primary metabolic organs.

The primary shortcoming of the paper is that the two HFDs were not controlled for caloric intake, carbohydrate content, sex of the mice, or the age of the mice at the onset of the diet. This is simply because, after discovering that HFD-1 induced the UPR, we wanted to confirm that this was not simply due to the extremely high fat content or the extremely low carbohydrate content. In fact, glucose deprivation has previously been shown to induce ER stress (12). It is thus possible that glucose deprivation, together with high levels of lipids, would have triggered the UPR. To eliminate this possibility, we wanted to test a more physiological diet and turned to our collaborators who had recently finished the study using HFD-2 looking at insulin resistance. Using the muscles, we confirmed that the UPR was activated in a lower-fat, higher-carbohydrate, "Western" diet. It was never our intention to compare the diets, only to confirm the presence of the UPR.

Recently, ER stress and UPR have gained major interest, as they have been proposed to be involved in the pathogenesis of diabetes (7), Parkinson's, Alzheimer's, and Huntington's disease (8, 14, 20) as well as hypoxia/ischemia-induced heart and brain damage (5). In diabetes, ER stress might contribute to pancreatic β-cell dysfunction and death as well as insulin resistance in the liver and adipose tissue (41). Despite its potential role in metabolic disease, there are a paucity of studies on ER stress in skeletal muscle.

In the first study, mice were placed on a diet containing 70% fat for a period of 6 wk. In this study, the effect of high-fat

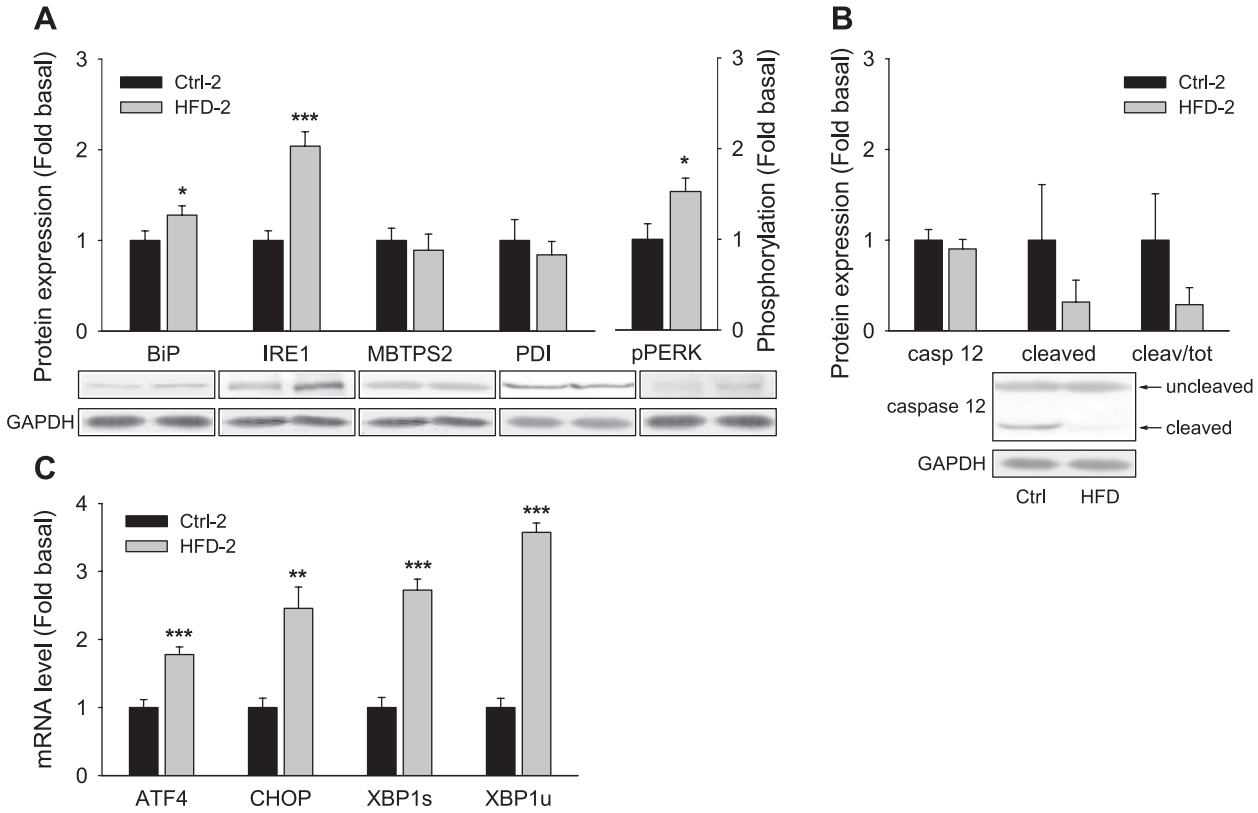

Fig. 4. 45% HFD-induced UPR in mouse skeletal muscle. *A*: protein expressions of BiP, IRE1α, MBTPS2, PDI, and phosphorylation of PERK. *B*: caspase-12 expression and cleavage in plantar flexor muscles after 20-wk HFD-2. *C*: mRNA level of ATF4, CHOP, XBP1s, and XBP1u in plantar flexor muscles after 20-wk HFD-2. Results are means ± SE. A value of 1 was arbitrarily assigned to control conditions to which HFD-2 were reported and expressed as fold basal. $*P < 0.05$, $**P < 0.01$, $***P < 0.001$ vs. Ctrl-2.

feeding on the UPR was measured separately in slow soleus and fast tibialis anterior muscles, with the greatest effects observed in the soleus. Whereas the tibialis anterior muscle is a voluntary muscle that is used sporadically, the soleus is a postural muscle in mice and is continuously active during standing and locomotion. In the soleus muscle, BiP, IRE1α, MBTPS2, and PERK protein levels were increased more than fivefold, whereas in the more phasically active tibialis anterior muscle these changes were less pronounced. The difference could be due to greater susceptibility of oxidative fibers to an HFD, an additive effect of contractile activity and HFD on ER stress or increased uptake of fatty acids in the soleus due to its higher blood flow and metabolic requirements.

Based on previous in vitro experiments, the UPR has been divided into three canonical pathways (21, 23, 35, 38, 48). They can be summarized as follows, emphasizing the markers measured in the present study: *1*) IRE1α and its downstream targets BiP and PDI; *2*) active ATF6 and the protease that cleaves it (i.e., MBTPS2) and its downstream targets BiP, CHOP, and XBP1; *3*) PERK and its downstream target ATF4. We cannot relate the changes in ER stress markers that we observed in vivo to the activation of any single pathway. For example, the increase in IRE1α expression was accompanied by an increase in BiP, whereas high-fat feeding in either the soleus or the tibialis anterior muscle did not affect PDI expression. In the same way, ATF4 mRNA was increased without any increase in PERK phosphorylation in the tibialis anterior muscle. This may mean that by sampling only at 6 wk we missed the transient changes, such as phosphorylation of PERK, and measured only the more stable changes such as ATF4 expression. Alternatively, 70% HFD for 6 wk leads to a general induction of the UPR rather than the activation of a specific sensor (ATF6, PERK, or IRE1α) and its downstream signaling, as would have been hypothesized from previous in vitro experiments.

When the UPR is not sufficient to cope with ER stress, inflammation and insulin resistance may develop. The 70% HFD increased plasma levels of cytokines such as IL-6 and IL-10, and this was associated with whole body glucose intolerance as demonstrated by the OGTT. In the same way, glucose intolerance was also induced after 20 wk of a 45% HFD. Taken together, these data confirm that a mild chronic inflammatory state and glucose intolerance were induced by high-fat feeding. However, the role of ER stress in the development of these physiological conditions has yet to be determined.

A more serious consequence of failure of the UPR is apoptosis. Caspase-12 has been proposed as a potential marker/mediator of ER stress-induced apoptosis (42). Increased caspase-12 activity has been identified in many neurodegenerative diseases, such as Parkinson's, Alzheimer's, or Huntington's diseases (8, 14, 20), which are believed to be the result of the fatal breakdown of the UPR. Caspase-12 is located at the ER membrane, and two different mechanisms have been proposed for its activation. The first involves an IRE1α-TRAF2 complex and is called "ER stress dependent" (50), while the

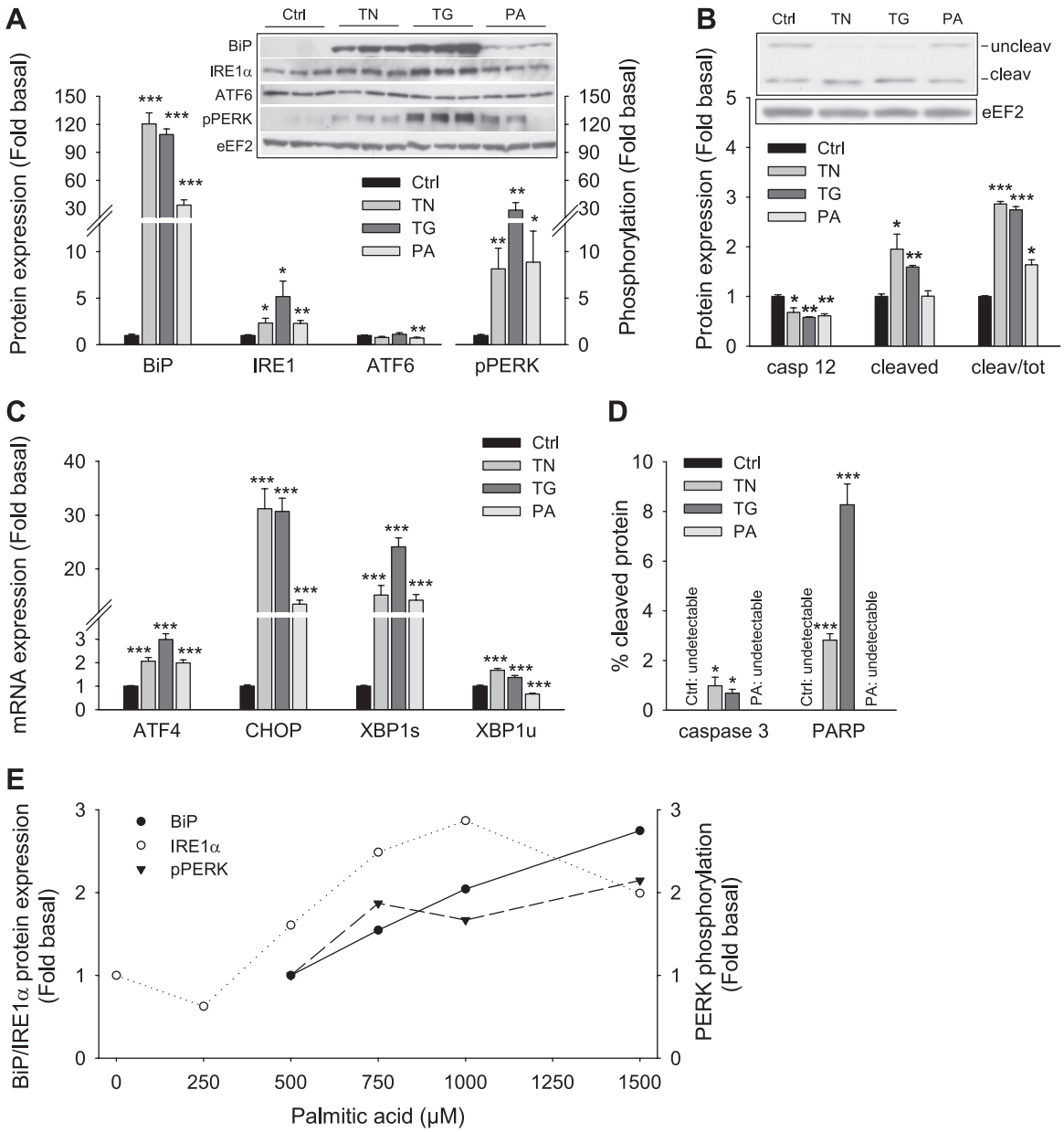

Fig. 5. Chemically induced UPR in C_2C_{12} myogenic cells. *A*: protein expression of BiP, IRE1α, ATF6, and phosphorylation of PERK. *B*: caspase-12 expression and cleavage. *C*: mRNA level of ATF4, CHOP, XBP1s, and XBP1u. *D*: %cleaved caspase-3 and cleaved poly ADP-ribose polymerase (PARP) after 17-h treatment with tunicamycin (TN, 1 μg/ml), thapsigargin (TG, 200 nM), or palmitic acid (PA, 1 mM) in C_2C_{12} cells. *E*: dose-response curves of BiP and IRE1α protein expression and of PERK phosphorylation to increasing concentrations of PA (0–1,500 μM). Results are means ± SE. A value of 1 was arbitrarily assigned to control conditions to which TN, TG, and PA values were reported and expressed as fold basal. $^*P < 0.05$, $^{**}P < 0.01$, $^{***}P < 0.001$ vs. Ctrl.

second, "ER stress independent", is associated with increase in calcium and caspase-7 activation (27). Despite an induction of the UPR, the 70% HFD did not change the expression of caspase-12 or its cleavage, suggesting that the degree of ER stress induced by 6-wk 70% HFD did not exceed the muscular capacity to refold/remove damaged proteins. Although no effect of HFD was observed on caspase-12, the basal cleavage pattern of this caspase seems to be different between soleus and tibialis anterior muscles. In the soleus muscle, a high percentage of the protein was in the cleaved form, whereas in the tibialis anterior, caspase-12 was found in its inactive total form. Since the soleus is a postural muscle, it experiences more frequent increases in intracellular calcium. The difference in caspase-12 cleavage may indicate that, in muscle, caspase-12 activation is mediated by calcium-dependent mechanisms rather than ER stress and may have other, apoptosis-independent, roles.

In the present study, C_2C_{12} cells were used to determine the functional effects of ER stress. Tunicamycin and thapsigargin were used as positive controls to which the effect of palmitic acid could be compared. All three compounds dramatically increased the expressions of BiP, IRE1α, and phospho-PERK at the protein level and CHOP, ATF4, and XBP1 spliced and unspliced at the mRNA level. Since the UPR is known to decrease protein synthesis and increase insulin resistance and apoptosis, we directly or indirectly measured each of

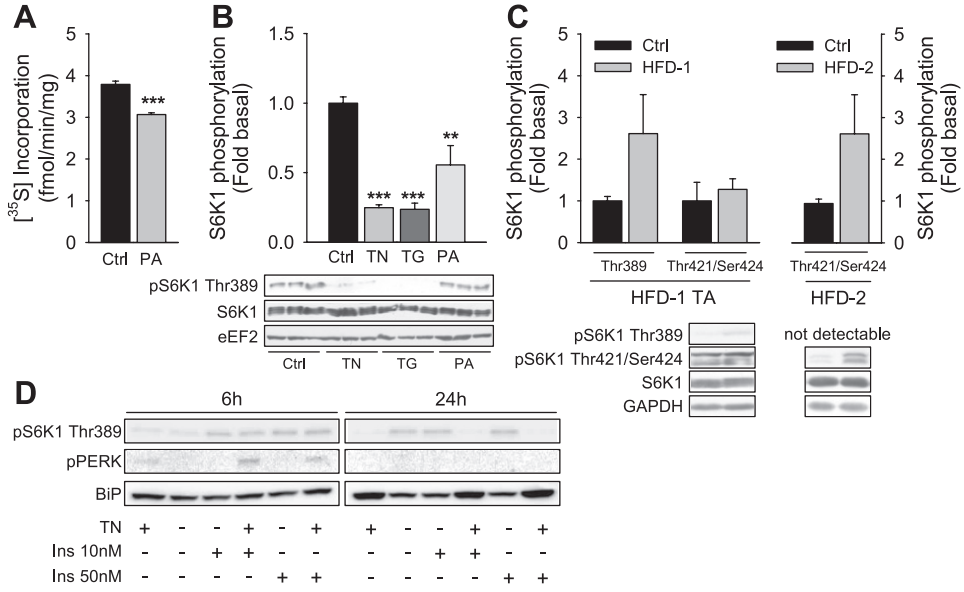

Fig. 6. ER stress reduces mTORC1 activity. *A*: palmitic acid (PA, 1 mM) reduces ^{35}S incorporation. *B*: PA (1 mM), tunicamycin (TN, 1 μg/μl), and thapsigargin (TG, 200 nM) decrease phosphorylation of S6K1 on Thr^{389}. *C*: phosphorylation of S6K1 on Thr^{389} and on Thr^{421}/Ser^{424} after 6-wk HFD-1 and after 20-wk HFD-2. *D*: phosphorylation of S6K1 (Thr^{389}) and PERK and expression of BiP after 6 and 24 h in C_2C_{12} cells treated with TN alone (1 μg/μl), insulin alone (Ins, 10 and 50 nM), or TN and insulin. S6K1, 70-kDa ribosomal protein S6 kinase; TA, tibialis anterior. Results are means ± SE. $^{**}P < 0.01$, $^{***}P < 0.001$ vs. Ctrl.

these events after palmitic acid treatment. Although palmitic acid clearly increased the UPR in myogenic cells, protein synthesis was the only physiological process that was affected over the 17 h of our study. This suggests that protein synthesis is the first process to be repressed in an effort to slow down the accumulation of newly synthesized proteins awaiting proper folding in the ER. A decrease in protein synthesis in skeletal muscle would, over time, be expected to lead to a decrease in lean body mass and, as a result, basal metabolic rate and glucose uptake in response to insulin. Whether the decrease in skeletal muscle protein synthesis in response to fat-induced ER stress plays a role in insulin resistance remains to be determined.

Recently, Sitnick et al. (39) have demonstrated that load-induced skeletal muscle hypertrophy is impaired in high-fat-fed mice. This decrease in hypertrophy was attributed to a decrease in ribosomal biogenesis and mTORC1 activation. mTORC1 is known to be physiologically inactivated only by the 5′-AMP-activated protein kinase (AMPK) (43), and during skeletal muscle overload AMPKα_1 is activated and slows muscle hypertrophy (24, 25). However, high-fat feeding decreases AMPK activity (2, 22), so a different mechanism must underlie the effect of HFD on skeletal muscle hypertrophy. To determine whether ER stress could contribute to this decrease in hypertrophy, we determined the rate of protein synthesis and the activation of mTORC1 following treatment with palmitic acid. Consistent with a role for ER stress in decreased load-induced hypertrophy, palmitic acid decreased both basal protein synthesis and mTORC1 activation. It should be mentioned that protein synthesis was not measured in vivo, and it thus remains to be determined whether high-fat feeding under the conditions used in the present study decreases basal, postprandial, and/or load-induced protein synthesis.

We sought to confirm that mTORC1 activity was also decreased after high-fat feeding in vivo. Contrary to our in vitro observations, S6K1 phosphorylation tended to be upregulated, in accord with previously published reports showing that HFD increases S6K1 phosphorylation in the basal state (1, 17). This finding is not incompatible with our in vitro data, since the extended HFDs used in the in vivo models will result in large-scale changes in the hormonal environment that may contribute to the regulation of mTORC1 activity. It is also possible that mTORC1 goes through cycles of activation-inactivation during periods of high circulating fatty acids and that the increase or decrease observed in S6K1 phosphorylation is dependent on the time of death. These cycles might be the result of decreases in mTORC1 activity due to ER stress followed by compensatory/feedback upregulation due to a resultant increase in IRS-1 signaling (45). The cycling of mTORC1 activity is illustrated by two studies from the same group using a genetic model of obesity and diabetes. At baseline, obese Zucker rats display either decreased (16) or increased (31) S6K1 phosphorylation compared with lean controls. The only difference between the two studies is the age of the rats at the time of the experiment, 12 (16) vs. 6 wk (31). Therefore, it seems that the time course of study is an important consideration when conducting studies on high-fat feeding and protein synthesis.

It should also be mentioned that the relationship between ER stress and mTORC1 is probably not unidirectional. A previous report has shown that hyperactivation of mTOR such as seen in tuberous sclerosis complex-deficient cells causes ER stress and activates the UPR (30). We directly tested whether 6 or 24 h of hyperactivation of mTORC1 by insulin was able to trigger the UPR in C_2C_{12} cells. In our conditions, insulin did not induce the UPR at any time point studied. Interestingly, tunicamycin activated the UPR before S6K1 phosphorylation decreased, suggesting that in C_2C_{12} cells the induction of ER stress precedes the impairment in mTORC1 activity.

In conclusion, we show that a high-fat diet activates the unfolded protein response in mouse skeletal muscle in vivo. In addition, in vitro palmitic acid, like other well-known ER stress inducers, triggered the unfolded protein response and also led to a decrease in protein synthesis and the activity of mTORC1. These findings suggest that components of the ER stress pathway might contribute to a decrease in muscle mass and the response to growth stimuli, as a result of metabolic syndrome.

ACKNOWLEDGMENTS

We thank Damien Naslain, Gang-Li An, and Vincent d'Harveng for technical assistance.

Current address for A. Philp and K. Baar: Dept. of Neurobiology, Physiology and Behavior, University of California, Davis, One Shields Ave., 181 Briggs Hall, Davis, CA 95616.

GRANTS

This work was supported by the Fonds National de la Recherche Scientifique (FNRS, Belgium), by the UCLouvain (F. S. R), and a project grant from the Wellcome Trust (077426). L. D is Postdoctoral Researcher, and P. D. C is Research Associate from the FRS (Fonds de la Recherche Scientifique)-FNRS, Belgium.

DISCLOSURES

No conflicts of interest are reported by the authors.

REFERENCES

1. **Anderson SR, Gilge DA, Steiber AL, Previs SF.** Diet-induced obesity alters protein synthesis: tissue-specific effects in fasted versus fed mice. *Metabolism* 57: 347–354, 2008.
2. **Beck Jorgensen S, O'Neill HM, Hewitt K, Kemp BE, Steinberg GR.** Reduced AMP-activated protein kinase activity in mouse skeletal muscle does not exacerbate the development of insulin resistance with obesity. *Diabetologia* 52: 2395–2404, 2009.
3. **Cani PD, Amar J, Iglesias MA, Poggi M, Knauf C, Bastelica D, Neyrinck AM, Fava F, Tuohy KM, Chabo C, Waget A, Delmee E, Cousin B, Sulpice T, Chamontin B, Ferrieres J, Tanti JF, Gibson GR, Casteilla L, Delzenne NM, Alessi MC, Burcelin R.** Metabolic endotoxemia initiates obesity and insulin resistance. *Diabetes* 56: 1761–1772, 2007.
4. **Cani PD, Knauf C, Iglesias MA, Drucker DJ, Delzenne NM, Burcelin R.** Improvement of glucose tolerance and hepatic insulin sensitivity by oligofructose requires a functional glucagon-like peptide 1 receptor. *Diabetes* 55: 1484–1490, 2006.
5. **Chen M, Won DJ, Krajewski S, Gottlieb RA.** Calpain and mitochondria in ischemia/reperfusion injury. *J Biol Chem* 277: 29181–29186, 2002.

5a. **Deldicque L, Atherton P, Patel R, Theisen D, Nielens H, Rennie MJ, Francaux M.** Effects of resistance exercise with and without creatine supplementation on gene expression and cell signaling in human skeletal muscle. *J Appl Physiol* 104: 371–378, 2008.

6. **Cnop M.** Fatty acids and glucolipotoxicity in the pathogenesis of Type 2 diabetes. *Biochem Soc Trans* 36: 348–352, 2008.
7. **Eizirik DL, Cardozo AK, Cnop M.** The role for endoplasmic reticulum stress in diabetes mellitus. *Endocr Rev* 29: 42–61, 2008.
8. **Forloni G, Terreni L, Bertani I, Fogliarino S, Invernizzi R, Assini A, Ribizzi G, Negro A, Calabrese E, Volonte MA, Mariani C, Franceschi M, Tabaton M, Bertoli A.** Protein misfolding in Alzheimer's and Parkinson's disease: genetics and molecular mechanisms. *Neurobiol Aging* 23: 957–976, 2002.
9. **Gilmore WJ, Kirby GM.** Endoplasmic reticulum stress due to altered cellular redox status positively regulates murine hepatic CYP2A5 expression. *J Pharmacol Exp Ther* 308: 600–608, 2004.
10. **Gregor MG, Hotamisligil GS.** Adipocyte stress: The endoplasmic reticulum and metabolic disease. *J Lipid Res,* 48: 1905–1914, 2007.
11. **Hu P, Han Z, Couvillon AD, Kaufman RJ, Exton JH.** Autocrine tumor necrosis factor alpha links endoplasmic reticulum stress to the membrane death receptor pathway through IRE1alpha-mediated NF-kappaB activation and down-regulation of TRAF2 expression. *Mol Cell Biol* 26: 3071–3084, 2006.
12. **Ikesugi K, Mulhern ML, Madson CJ, Hosoya K, Terasaki T, Kador PF, Shinohara T.** Induction of endoplasmic reticulum stress in retinal pericytes by glucose deprivation. *Curr Eye Res* 31: 947–953, 2006.
13. **Ikezoe K, Nakamori M, Furuya H, Arahata H, Kanemoto S, Kimura T, Imaizumi K, Takahashi MP, Sakoda S, Fujii N, Kira J.** Endoplasmic reticulum stress in myotonic dystrophy type 1 muscle. *Acta Neuropathol* 114: 527–535, 2007.
14. **Imaizumi K, Miyoshi K, Katayama T, Yoneda T, Taniguchi M, Kudo T, Tohyama M.** The unfolded protein response and Alzheimer's disease. *Biochim Biophys Acta* 1536: 85–96, 2001.
15. **Kaneto H, Matsuoka TA, Nakatani Y, Kawamori D, Miyatsuka T, Matsuhisa M, Yamasaki Y.** Oxidative stress, ER stress, and the JNK pathway in type 2 diabetes. *J Mol Med* 83: 429–439, 2005.
16. **Katta A, Karkala SK, Wu M, Meduru S, Desai DH, Rice KM, Blough ER.** Lean and obese Zucker rats exhibit different patterns of p70s6 kinase regulation in the tibialis anterior muscle in response to high-force muscle contraction. *Muscle Nerve* 39: 503–511, 2009.
17. **Khamzina L, Veilleux A, Bergeron S, Marette A.** Increased activation of the mammalian target of rapamycin pathway in liver and skeletal muscle of obese rats: possible involvement in obesity-linked insulin resistance. *Endocrinology* 146: 1473–1481, 2005.
18. **Kim DS, Jeong SK, Kim HR, Chae SW, Chae HJ.** Effects of triglyceride on ER stress and insulin resistance. *Biochem Biophys Res Commun* 363: 140–145, 2007.
19. **Kim I, Xu W, Reed JC.** Cell death and endoplasmic reticulum stress: disease relevance and therapeutic opportunities. *Nat Rev Drug Discov* 7: 1013–1030, 2008.
20. **Kudo T, Katayama T, Imaizumi K, Yasuda Y, Yatera M, Okochi M, Tohyama M, Takeda M.** The unfolded protein response is involved in the pathology of Alzheimer's disease. *Ann NY Acad Sci* 977: 349–355, 2002.
21. **Lai E, Teodoro T, Volchuk A.** Endoplasmic reticulum stress: signaling the unfolded protein response. *Physiology (Bethesda)* 22: 193–201, 2007.
22. **Liu Y, Wan Q, Guan Q, Gao L, Zhao J.** High-fat diet feeding impairs both the expression and activity of AMPKa in rats' skeletal muscle. *Biochem Biophys Res Commun* 339: 701–707, 2006.
23. **Malhotra JD, Kaufman RJ.** The endoplasmic reticulum and the unfolded protein response. *Semin Cell Dev Biol* 18: 716–731, 2007.
24. **McGee SL, Mustard KJ, Hardie DG, Baar K.** Normal hypertrophy accompanied by phosphoryation and activation of AMP-activated protein kinase alpha1 following overload in LKB1 knockout mice. *J Physiol* 586: 1731–1741, 2008.
25. **Mounier R, Lantier L, Leclerc J, Sotiropoulos A, Pende M, Daegelen D, Sakamoto K, Foretz M, Viollet B.** Important role for AMPKalpha1 in limiting skeletal muscle cell hypertrophy. *FASEB J* 23: 2264–2273, 2009.
26. **Nagaraju K, Casciola-Rosen L, Lundberg I, Rawat R, Cutting S, Thapliyal R, Chang J, Dwivedi S, Mitsak M, Chen YW, Plotz P, Rosen A, Hoffman E, Raben N.** Activation of the endoplasmic reticulum stress response in autoimmune myositis: potential role in muscle fiber damage and dysfunction. *Arthritis Rheum* 52: 1824–1835, 2005.
27. **Nakagawa T, Yuan J.** Cross-talk between two cysteine protease families. Activation of caspase-12 by calpain in apoptosis. *J Cell Biol* 150: 887–894, 2000.
28. **Oyadomari S, Harding HP, Zhang Y, Oyadomari M, Ron D.** Dephosphorylation of translation initiation factor 2alpha enhances glucose tolerance and attenuates hepatosteatosis in mice. *Cell Metab* 7: 520–532, 2008.
29. **Ozcan U, Cao Q, Yilmaz E, Lee AH, Iwakoshi NN, Ozdelen E, Tuncman G, Gorgun C, Glimcher LH, Hotamisligil GS.** Endoplasmic reticulum stress links obesity, insulin action, and type 2 diabetes. *Science* 306: 457–461, 2004.
30. **Ozcan U, Ozcan L, Yilmaz E, Duvel K, Sahin M, Manning BD, Hotamisligil GS.** Loss of the tuberous sclerosis complex tumor suppressors triggers the unfolded protein response to regulate insulin signaling and apoptosis. *Mol Cell* 29: 541–551, 2008.
31. **Paturi S, Gutta AK, Kakarla SK, Katta A, Arnold EC, Wu M, Rice KM, Blough ER.** Impaired overload-induced hypertrophy in obese Zucker rat slow-twitch skeletal muscle. *J Appl Physiol* 108: 7–13, 2010.
32. **Pedersen BK, Febbraio MA.** Muscle as an endocrine organ: focus on muscle-derived interleukin-6. *Physiol Rev* 88: 1379–1406, 2008.
33. **Pedersen M, Bruunsgaard H, Weis N, Hendel HW, Andreassen BU, Eldrup E, Dela F, Pedersen BK.** Circulating levels of TNF-alpha and IL-6-relation to truncal fat mass and muscle mass in healthy elderly individuals and in patients with type-2 diabetes. *Mech Ageing Dev* 124: 495–502, 2003.
34. **Peter A, Weigert C, Staiger H, Machicao F, Schick F, Machann J, Stefan N, Thamer C, Haring HU, Schleicher E.** Individual stearoyl-coa desaturase 1 (SCD1) expression modulates er stress and inflammation in human myotubes and is associated with skeletal muscle lipid storage and insulin sensitivity in vivo. *Diabetes* 58: 1757–1765, 2009.
35. **Ron D, Walter P.** Signal integration in the endoplasmic reticulum unfolded protein response. *Nat Rev Mol Cell Biol* 8: 519–529, 2007.
36. **Sakaki K, Wu J, Kaufman RJ.** Protein kinase Ctheta is required for autophagy in response to stress in the endoplasmic reticulum. *J Biol Chem* 283: 15370–15380, 2008.

37. **Scheuner D, Kaufman RJ.** The unfolded protein response: a pathway that links insulin demand with beta-cell failure and diabetes. *Endocr Rev* 29: 317–333, 2008.
38. **Schroder M, Kaufman RJ.** The mammalian unfolded protein response. *Annu Rev Biochem* 74: 739–789, 2005.
39. **Sitnick M, Bodine SC, Rutledge JC.** Chronic high fat feeding attenuates load-induced hypertrophy in mice. *J Physiol* 587: 5753–5765, 2009.
40. **Srinivasan S, Ohsugi M, Liu Z, Fatrai S, Bernal-Mizrachi E, Permutt MA.** Endoplasmic reticulum stress-induced apoptosis is partly mediated by reduced insulin signaling through phosphatidylinositol 3-kinase/Akt and increased glycogen synthase kinase-3beta in mouse insulinoma cells. *Diabetes* 54: 968–975, 2005.
41. **Sundar Rajan S, Srinivasan V, Balasubramanyam M, Tatu U.** Endoplasmic reticulum (ER) stress & diabetes. *Indian J Med Res* 125: 411–424, 2007.
42. **Szegezdi E, Fitzgerald U, Samali A.** Caspase-12 and ER-stress-mediated apoptosis: the story so far. *Ann NY Acad Sci* 1010: 186–194, 2003.
43. **Thomson DM, Fick CA, Gordon SE.** AMPK activation attenuates S6K1, 4E-BP1, and eEF2 signaling responses to high-frequency electrically stimulated skeletal muscle contractions. *J Appl Physiol* 104: 625–632, 2008.
44. **Tirasophon W, Lee K, Callaghan B, Welihinda A, Kaufman RJ.** The endoribonuclease activity of mammalian IRE1 autoregulates its mRNA and is required for the unfolded protein response. *Genes Dev* 14: 2725–2736, 2000.
45. **Tremblay F, Marette A.** Amino acid and insulin signaling via the mTOR/p70 S6 kinase pathway. A negative feedback mechanism leading to insulin resistance in skeletal muscle cells. *J Biol Chem* 276: 38052–38060, 2001.
46. **Ueda K, Kawano J, Takeda K, Yujiri T, Tanabe K, Anno T, Akiyama M, Nozaki J, Yoshinaga T, Koizumi A, Shinoda K, Oka Y, Tanizawa Y.** Endoplasmic reticulum stress induces Wfs1 gene expression in pancreatic beta-cells via transcriptional activation. *Eur J Endocrinol* 153: 167–176, 2005.
47. **Vattemi G, Engel WK, McFerrin J, Askanas V.** Endoplasmic reticulum stress and unfolded protein response in inclusion body myositis muscle. *Am J Pathol* 164: 1–7, 2004.
48. **Wu J, Kaufman RJ.** From acute ER stress to physiological roles of the Unfolded Protein Response. *Cell Death Differ* 13: 374–384, 2006.
49. **Yamamoto K, Ichijo H, Korsmeyer SJ.** BCL-2 is phosphorylated and inactivated by an ASK1/Jun N-terminal protein kinase pathway normally activated at G(2)/M. *Mol Cell Biol* 19: 8469–8478, 1999.
50. **Yoneda T, Imaizumi K, Oono K, Yui D, Gomi F, Katayama T, Tohyama M.** Activation of caspase-12, an endoplastic reticulum (ER) resident caspase, through tumor necrosis factor receptor-associated factor 2-dependent mechanism in response to the ER stress. *J Biol Chem* 276: 13935–13940, 2001.
51. **Yoshida H, Matsui T, Yamamoto A, Okada T, Mori K.** XBP1 mRNA is induced by ATF6 and spliced by IRE1 in response to ER stress to produce a highly active transcription factor. *Cell* 107: 881–891, 2001.
52. **Yoshiuchi K, Kaneto H, Matsuoka TA, Kohno K, Iwawaki T, Nakatani Y, Yamasaki Y, Hori M, Matsuhisa M.** Direct monitoring of in vivo ER stress during the development of insulin resistance with ER stress-activated indicator transgenic mice. *Biochem Biophys Res Commun* 366: 545–550, 2008.
53. **Zenobi PD, Holzmann P, Glatz Y, Riesen WF, Froesch ER.** Improvement of lipid profile in type 2 (non-insulin-dependent) diabetes mellitus by insulin-like growth factor I. *Diabetologia* 36: 465–469, 1993.
54. **Zhang K, Kaufman RJ.** Protein folding in the endoplasmic reticulum and the unfolded protein response. *Handb Exp Pharmacol*: 69–91, 2006.